Synthesis and Characterization of Cu/Fe Doping and Co-Doping in the Structure of PbS Semiconductor Material

Yirgalem Bekele Wami

A Thesis Submitted to the Department of Applied Physics

School of Applied Natural Science Office of Graduate

Studies Adama Science and Technology University

June 2024

Adama, Ethiopia

Synthesis and Characterization of Cu/Fe Doping and Co-Doping in the Structure of PbS Semiconductor Material

Yirgalem Bekele Wami

Adivsor: Dr. Fekadu Tolessa

A Thesis Submitted to the Department of Applied Physics

School of Applied Natural Science Office of Graduate

Studies Adama Science and Technology University

June 2024

Adama, Ethiopia

Declaration

I hereby declare that this Master Thesis entitled "Synthesis and Characterization of Cu/Fe Doping and Co-Doping in the Structure of PbS Semiconductor Material" is my original work. That is, it has not been submitted for the award of any academic degree, diploma or certificate in any other university. All sources of materials that are used for this thesis have been duly acknowledged through citation.

Yirgalem Bekele Wami		
Name of student	Signature	Date

Recommendation

We, the advisor of this thesis, hereby certify that we have read the revised ver sion of the thesis entitled "Synthesis and Characterization of Cu/Fe Doping and Co-Doping in the Structure of PbS Semiconductor Material" prepared under our guidance by Yirgalem Bekele submitted in partial fulfillment of the requirements for the degree of Mater's of Science in Condensed Matter of Physics. Therefore, we recommend the submission of revised version of the thesis to the department following the applicable procedures.

Dr. Fekadu Tolessa	_____	_____
Advisor	Signature	Date
Dr. Gashaw Beyene	_____	_____
Co-Advisor	Signature	Date

Approval Page

We, the advisors of the thesis entitled "Synthesis and Characterization of Cu/Fe Doping and Co-Doping in the Structure of PbS Semiconductor Material" and developed by Yirgalem Bekele, hereby certify that the recommendation and sug gestions made by the board of examiners are appropriately incorporated into the final version of the thesis.

Dr. Fekadu Tolessa	_____	_____
Advisor	Signature	Date
Dr. Gashaw Beyene	_____	_____
Co-Advisor	Signature	Date

We, the undersigned, members of the Board of Examiners of the thesis by Yirgalem Bekele have read and evaluated the thesis entitled "Synthesis and Characterization of Cu/Fe Doping and Co-Doping in the Structure of PbS Semiconductor Material" and examined the candidate during open defense. This is, therefore, to certify that the thesis is accepted for partial fulfillment of the requirement of the degree of Master of Science in Condensed Matter of Physics.

_____	_____	_____
Chair Person	Signature	Date
_____	_____	_____
Internal Examiner	Signature	Date
_____	_____	_____
External Examiner	Signature	Date
_____	_____	_____
Office of postgraduate Studies	Signature	Date

ACKNOWLEDGMENT

Above all, I would like to thank the almighty God; Next, I would like to give a deepest gratitude to my advisor Dr.Fekadu Tolessa for his guidance and contribution of suggestions, I am heartily thankful. I would like to give a deepest gratitude to Adama Science and Technology University opening this program, School of Applied Natural Science and Department of Applied Physics. Also I would like to thank my husband Tekle Wakene for supporting me in all aspects.

Abstract

This thesis work explores the synthesis and characterization of copper (Cu) and iron (Fe) doped, as well as co-doped, lead sulfide (PbS) nanoparticles, focusing on their potential applications in semiconductor technology. PbS nanoparticles were synthesized using experimental chemical Synthesizing sol-gel method, followed by the incorporation of Cu and Fe dopants through a controlled doping and co doping process. The structural, morphological, and optical properties of the synthesized nanoparticles were thoroughly analyzed using X-ray diffraction (XRD), scanning electron microscopy (SEM), Photoluminescence (PL). XRD analysis confirmed the crystalline structure of the PbS nanoparticles and indicated successful incorporation of Cu and Fe ions into the PbS lattice, evidenced by slight shifts in the diffraction peaks. SEM images revealed uniform particle distribution and size, optical properties were assessed through PL, demonstrating a notable change in the band gap energy due to doping, which can be tuned by doping co-doping. The findings highlight the influence of Cu and Fe doping on the structural and optical properties of PbS nanoparticles, suggesting their potential for enhancing the performance of semiconductor devices. These doped nanoparticles exhibit modified opto-electrical characteristics, making them suitable for applications in photovoltaic cells, sensors, and other optoelectronic devices. The experimental approach outlined provides a reliable method for the synthesis and characterization of doped and co-doped semiconductor nanoparticles, paving the way for further research and development in advanced nano-materials.

List of Acronyms

NPS	Nanoparticles
PbS	Lead sulfide
UV	ultra-violet
XRD	X-ray diffraction
TGA	Thermal Gravimetric Analysis
DTA	Differential Thermal Analysis
SDS	sodium dodecyl sulfate
TEM	Transmission Electron Microscopy
PVP	Poly Vinyl Pyrrolidone
FWHN	Full width at half maximum
SEM	Scanning Electro-microscopy
EDAX	Energy Dispersive X-Ray Spectroscopy
FTIR	Fourier transform infrared
IR	Infra-Red
DI	Di-ionized
LED	Light Emitting Diode
VLSI	Very Large Scale Integrated circuit
LSI	Large Scale Integrated circuit
IC	Integrated Circuit
AC	Alternating Current
DC	Direct Current
PH	Power of Hydrogen
ICDD	International Centre for Diffraction Data

Contents

List of Figures

List of Tables

Chapter 1

Introduction

The origin of semiconductors dates back to the creation of the rectifier (AC-DC converter) in 1874. Later on, in 1947, at Bell Laboratories in the United States, Bardeen and Brattain devised the point-contact transistor, followed by Shockley inventing the junction transistor in 1948. This marked the beginning of the transistor era. Additionally, in 1946, the University of Pennsylvania in the US constructed a computer utilizing vacuum tubes (Yoshida et al, 2022). The computer was immensely sizable, with its vacuum tubes taking up the entire building, consuming a significant amount of electricity, and generating excessive heat. Subsequently, the groundbreaking transistor calculator (computer) was created, leading to a rapid advancement in computer technology. In 1956, the Nobel Prize in Physics was collectively bestowed upon Shockley, Bardeen, and Brattain for their significant contributions to semiconductor research and the innovation of the transistor (Riordan et al, 1999).

After the creation of the transistor, the semiconductor industry experienced swift growth. By 1957, its scale had surpassed 100 million dollars. Subsequently, in 1959, Kilby of Texas Instruments and Noyce of Fairchild Semiconductor in the US developed the bipolar integrated circuit (ICs), further propelling advancements in the field (DeBenedictis et al, 2017). This innovation had a significant influence on the semiconductor history, signifying the beginning of the IC era. Due to its compact size and lightweight nature, the IC found broad applications in various electrical devices. In 1967, Texas Instruments created the electronic desktop calculator (the calculator) employing IC technology (Wang and Zheng, 2023). In

Japan, manufacturers of electronic equipment launched calculators in rapid succession, sparking intense "calculator wars" that persisted until the late 1970s. IC integration progressed, leading to the development of the large-scale integrated circuit (LSI). Technological advancements have continued to evolve as noted by Unno and Iwai in 1999. The Very-Large-Scale Integration (VLSI) technology, with chip capacities ranging from 100 thousand to 10 million electronic components, emerged in the 1980s. Subsequently, in the 1990s, the Ultra-Large-Scale Integration (ULSI) technology, incorporating over 10 million electronic components per chip, was introduced. (Kato et al, 1991). During the 2000s, the system LSI, a multifunction LSI consolidating multiple functions into a single chip, entered full-scale production. As IC technology advances towards higher performance and increased functionality, its application scope broadens significantly. Today, semiconductors play a crucial role in various aspects of our society, supporting everyday activities. The early semiconductor devices, such as crystal detectors, used galena, notably seen in German physicist Ferdinand Braun's crystal detector in 1874 and Indian physicist Jagadish Chandra Bose's radio crystal detector in 1901 (Patil et al, 2021). The point-contact crystal detector played a critical role in microwave radio systems as existing vacuum tube devices were incapable of serving as detectors beyond approximately 4000 MHz. Advanced radar systems heavily depended on the swift response provided by crystal detectors. Extensive research and development efforts focused on silicon materials during the war aimed at creating detectors with consistent quality. (Zulehner et al, 2000).

A semiconductor is a material with electrical conductivity that falls between that of a conductor, like copper, and an insulator, such as glass. Its resistivity decreases as temperature increases, whereas metals exhibit the opposite behavior. By introducing impurities (doping) into the crystal structure, the conducting characteristics of semiconductors can be purposely modified. When two differently doped regions coexist within the same crystal, a semiconductor junction forms. The interactions of charge carriers, including electrons-ions, and electron-holes, form the foundation of diodes, transistors, and advanced

electronics. The contemporary comprehension of semiconductor properties relies on quantum physics to elucidate the motion of charge carriers within a crystal lattice (Enderlein and H. et al, 1997). Doping significantly boosts the quantity of charge carriers within the crystal. If a doped semiconductor harbors free holes, it is classified as "p-type," whereas if it encompasses free electron it is termed as “n-type”.

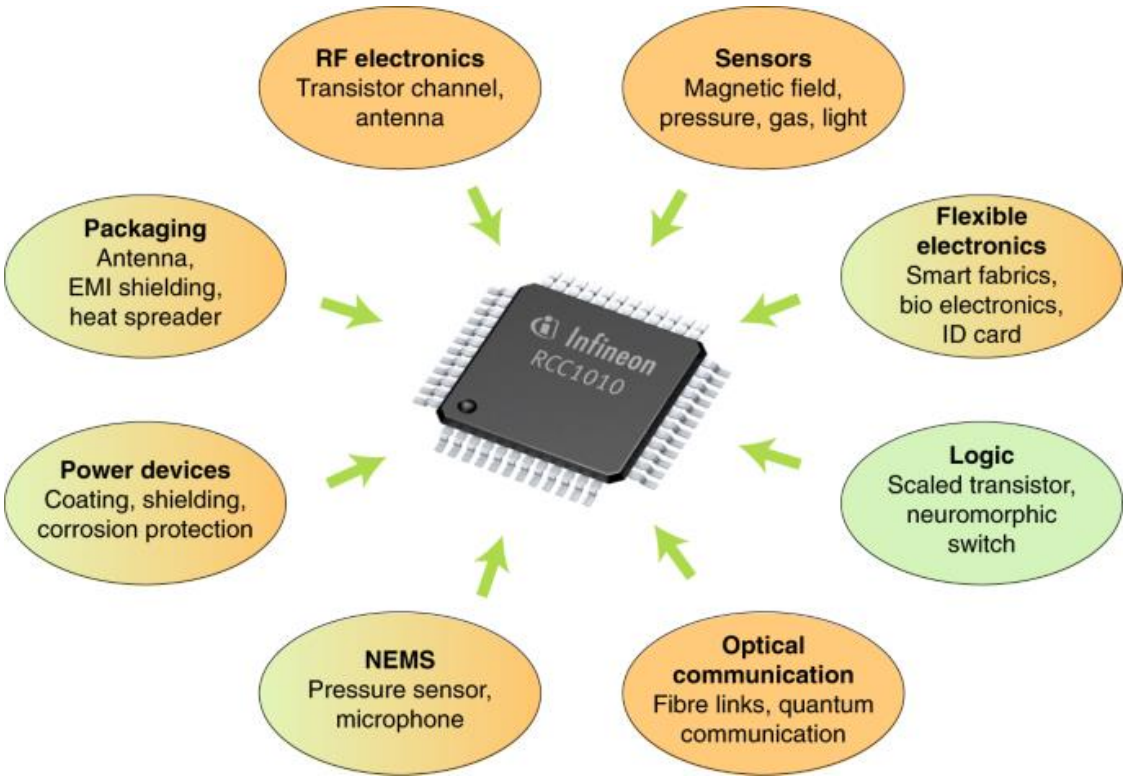

Figure 1.1: Semiconductor Application

Semiconductor materials utilized in electronic devices undergo precise doping conditions to regulate the concentration and distribution of p-type and n-type dopants. A single semiconductor device crystal can host numerous p- and n-type regions, with the p-n junctions between these areas governing the beneficial electronic characteristics. By utilizing a hot-point probe, it is possible to swiftly ascertain whether a semiconductor sample is of p- or n-type. (Teng et al., 2018). The initial practical utilization of semiconductors in electronics dates back to 1904 with the introduction of the cat's whisker detector, a rudimentary semiconductor diode implemented in early radio receivers.

Semiconductors' conductivities can be readily adjusted by introducing impurities into their crystal lattice. The method of incorporating regulated impurities into a semiconductor is called doping. The quantity of impurity, or dopant, introduced into an intrinsic (pure) semiconductor alters its conductivity level. (Schubert et al, 2015). Semiconductors that have been doped are known as extrinsic semiconductors. The introduction of impurities into pure semiconductors allows for the manipulation of electrical conductivity by factors of thousands or even millions. Semiconductors exhibit a distinctive electrical conductive characteristic lying between that of conductors and insulators. (Mott et al 1972), The distinctions among these materials can be comprehended through the concept of quantum states for electrons, each capable of accommodating either zero or one electron (as per the Pauli exclusion principle). These states are related to the electronic band structure of the material. Electrical conductivity emerges from the existence of electrons in delocalized states that extend throughout the material. Nonetheless, for electron transport to occur, a state must be partially occupied, hosting an electron intermittently. (Jaiswal et al, 2006). In materials where a state is constantly occupied by an electron, it becomes inert, hindering the flow of other electrons through that state. Enhanced conductivity in a material results from having numerous partially filled states and a high degree of state delocalization.

Metals, known for their conductivity, harbor multiple partially occupied states with energies close to their Fermi level. In contrast, insulators possess few partially filled states, with their Fermi levels situated within band gaps containing minimal energy states for electron occupancy. Notably, insulators can transition to a conductive state with increased temperature: heating supplies the required energy to propel some electrons across the band gap, creating partially filled states in both the valence band (below the band gap) and the conduction band (above the band gap). An intrinsic semiconductor exhibits a band gap smaller than that of an insulator, enabling a substantial number of electrons to be excited across the band gap at room temperature. (Chaves et al., 2020).

A pure semiconductor, while not particularly efficient, falls between being a good insulator and a good conductor. Nonetheless, a key attribute of semiconductors (as well as certain insulators denoted as semi-insulators) is their modifiable and controllable conductivity through impurity doping and electric field gating. Through doping and gating, either the conduction or valence band can be brought closer to the Fermi level, significantly enhancing the number of partially occupied states.

Certain semiconductor materials with wider band gaps are sometimes labeled as semi-insulators. In their un-doped state, these materials exhibit electrical conductivity levels closer to insulators. However, through doping, they can be rendered as functional as semiconductors or even utilized as insulating materials for specific applications, all while serving as wide-band gap semiconductors in other scenarios.

1.2 Statement of the Problem

Lead sulfide (PbS) nanoparticles exhibit remarkable adaptability and potential for use in both conventional optical devices and the emerging field of nano-electronics and nano-optoelectronics due to their unique structural and size-dependent characteristics. Despite being a subject of intensive research, a comprehensive assessment of the existing literature on PbS nanoparticles has

not been compiled to date. The primary driver behind the exploration of lead sulfide (PbS) properties is its significant role as a cornerstone in modern semiconductor optoelectronics. Undoubtedly, presenting a comprehensive overview of the published studies will not only advance research in the field of PbS by doping Cu, and Fe and co-dope PbS with Cu, Fe. This research paper delves into the synthesis and characterizes structural, electronic, and optical features of doped and co-doped PbS nanoparticles within the context of recent advancements in nanotechnology.

1.3 Objectives

1.3.1 General Objective

The general objective of this study is to Synthesis and Characterization of Cu/Fe Doping and Co-Doping in the Structure of PbS Semiconductor Material using experimental method.

1.3.2 Specific Objectives

The specific objectives of this work are to:-

- Synthesis and characterize the doping and co-doping of Cu/Fe PbS.
- Study the crystal structure of doped Cu, Fe and co-dope with PbS.
- Analyze the band gap energy of CuPbS, FePbS and CuPbFeS.

1.4 Significance of the Study

Over the last two decades, substantial experimental and theoretical endeavors have been dedicated to exploring the intricacies of co-doping in semiconductor materials. The outcomes of these investigations aim to enhance the capabilities of lead sulfide (PbS) nanoparticles doped with elements like copper (Cu), iron (Fe), and co-dopants (Cu, Fe) for future optoelectronic applications. This study focuses on improving the solubility of dopants, enhancing the stability of desired defects, and optimizing the performance of PbS-based devices. By incorporating dopants into semiconductor materials, chemical applications enable the modification of electronic properties, offering a range of benefits essential for human well-being such as healthcare, warmth, sustenance, illumination, attire, shelter, and transportation. The co-doping technique serves as a valuable tool to adjust dopant concentrations, electronic attributes characteristics of semiconductors.

1.5 Scope of the Study

This research work will be delimited to chemical synthesis by sol-gel method. The doped and co-doped nanoparticles can be characterized by using XRD, PL, and SEM, Furthermore, the application of the doped and co-doped nanoparticle material have range with an amount a band gap, crystal structure of optoelectronic semiconductor materials.

In this chapter the background of the study, statement of the problem have been presented further the study aims, associated objective, the scope of the study, the significance of the study and the organization of the thesis to achieve these objectives have briefly been presented. In the next chapter, the literature review and the gaps in the different research papers will be presented.

Chapter 2

Review Literature

In this chapter the theoretical aspect of the concept of semiconducting nanoparticles synthesizing approaches of lead-sulfide nanoparticles reviewed in the litera- ture; The properties, synthesizing approach characterization techniques, using lead sulfide by doping and co-dopant application were described.

2.1 Semiconductor nanoparticles

Semiconductor nanoparticles are recognized for exhibiting a rich array of quantum phenomena and demonstrating distinctive material properties that vary depending on their size. These materials display characteristics that lie in between those of metals and nonmetals, leading to their widespread utilization across different fields. When the size of the nanoparticles is altered, substantial alterations occur in their electronic and optical properties owing to the confinement of electrons and holes in three dimensions as the particle size approaches the Bohr radius of an excitation.

Semiconductor nanoparticles possess a wide band-gap, and as a result, they display significant changes in their properties through band-gap tuning. This characteristic makes them highly suitable for applications in areas such as photo catalysis, photo-optics, and electronic devices. They hold great promise for applications in water-splitting due to their appropriate band-gap and band edge positions (Satvekar et al., 2015).

2.1.1 Electronic Structure of Semiconductors

The electronic characteristics of a semiconductor play a vital role in device functionalities. These attributes are influenced by factors like the crystal structure, the bonding type within the material, and ultimately, the electron wave functions. To grasp these fundamental concepts, let's focus on examples from the prominent class of semiconductors known as diamond-type semiconductors, including silicon, germanium, and gallium arsenide.

By examining these examples, we aim to provide insight into the band structures of these materials and illustrate how this structure dictates crucial properties of the crystal. (Kim et al., 2012).

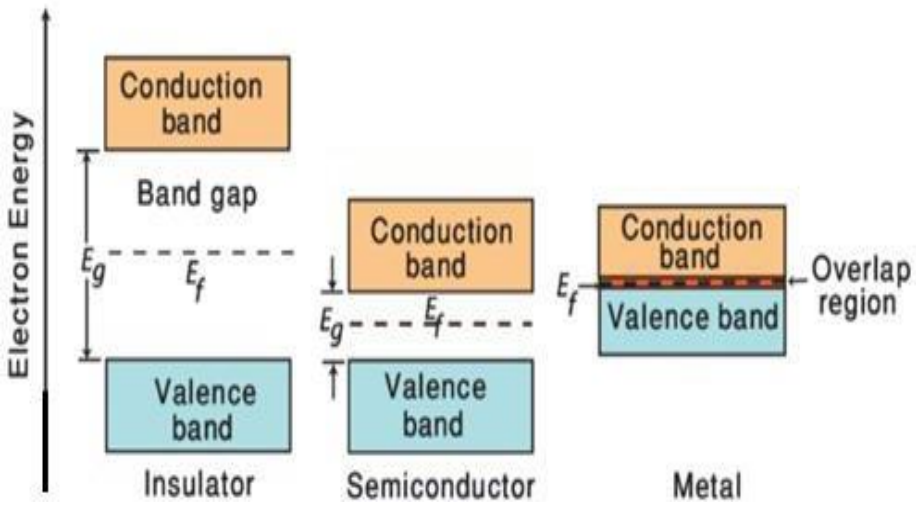

Figure 2.1: Electron Energy Band gap

The band gap of a semiconductor represents the minimum energy needed to move an electron from a bound state to a free state where it can conduct electricity. The band structure of a semiconductor illustrates the energy levels of electrons on the y-axis, typically depicted as a "band diagram." Within this structure, the lower energy level is identified as the "valence band" (EV), where electrons are bound, while the energy level allowing electron mobility is termed the "conduction band" (EC).

The energy gap (EG) refers to the distinction in energy between the valence and conduction bands, signifying the band gap. Therefore, the energy band gap denotes the minimum energy alteration essential to transition an electron from a bound state to a free state for conduction purposes. (Xu et al, 2000). When an electron is excited into the conduction band within a semiconductor, it gains the freedom to traverse the material and partake in electrical conduction. However, this electron excitation to the conduction band initiates another conduction mechanism. By moving to the conduction band, the electron leaves a void in the valence band that can be occupied by an electron from a neighboring atom. This sequential movement of electrons creates what is known as a "hole," representing a space where an electron used to be.

As electrons move to fill these holes, they leave behind new holes, leading to a continuous process of hole migration through the crystal lattice. This movement of positively charged "holes" can be visualized as the motion of a positively charged particle through the semiconductor's structure. Consequently, the excitation of an electron into the conduction band engenders not only an electron in the conduction band but also a corresponding hole in the valence band. Both the electrons in the conduction band and the holes in the valence band are capable of participating in electrical conduction and are commonly referred to as "carriers".

2.1.2 Lead Sulfide (PbS) Semiconductor

Lead sulfide (PbS) is a significant IV-VI semiconductor material known for its direct band gap, making it highly appealing due to its adjustable particle size. In its bulk form, lead sulfide stands out as one of the most favored IV-VI group semiconductors, possessing a narrow direct band gap typically around 0.42 eV at room temperature and 0.286 eV at 4.2 K. The optical and electronic characteristics of lead sulfide stem from the quantum confinement effect, which elucidates electron behavior in terms of energy levels, potential wells, valence bands, conduction bands, and electron energy band gaps. (Parveen et al, 2018). The

quantum confinement effect is observed when the size of the particle is too small to be comparable to the wavelength of the electron.

Figure 2.2: Lead Sulfide powder

2.2 Doping Semiconductors

In the realm of semiconductor production, doping involves deliberately introducing impurities into an intrinsic semiconductor to alter its electrical, optical, and structural characteristics. The doped material transforms into an extrinsic semiconductor through this process. Even a small quantity of dopant atoms can significantly impact a semiconductor's conductivity. For instance, when approximately one dopant atom is added per 100 million atoms, the doping is categorized as low or light. Conversely a higher concentration of dopant atoms, around one per ten thousand atoms, leads to what is known as high or heavy doping.

This distinction in doping levels is often denoted as n+ for n-type doping or p+ for p-type doping. If a semiconductor is doped to such an extent that it behaves more like a conductor than a semiconductor, it is termed a degenerate semiconductor. Meanwhile, an i-type semiconductor arises when a semiconductor is doped evenly with p-type and n-type dopants in equal quantities.

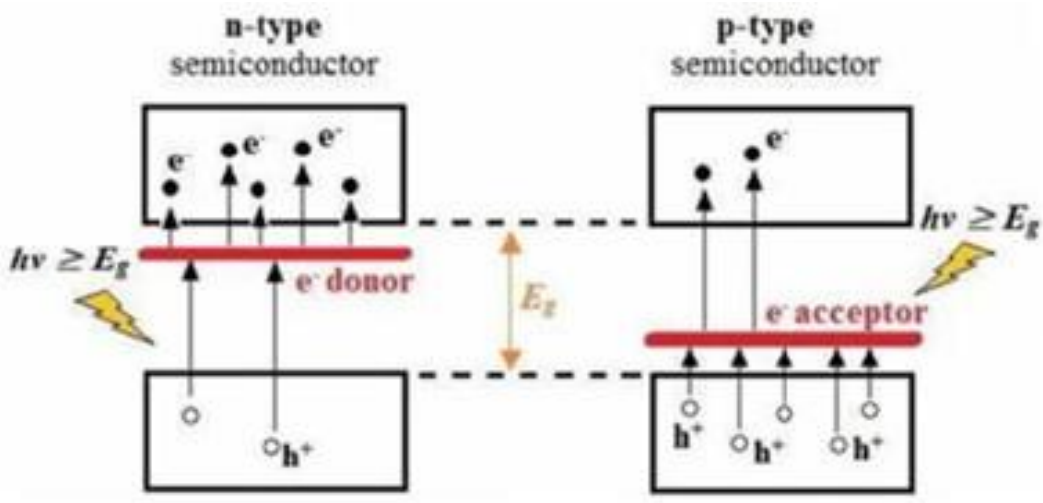

Figure 2.3: Doped semiconductor

2.2.1 Co-doping semiconductors

Co-doping is a highly effective strategy utilized for adjusting dopant populations and enhancing electronic properties in semiconductors. This approach aims to improve dopant solubility and enhance the stability of desired defects within the material. Over the last two decades, substantial experimental and theoretical research has been dedicated to investigating the attributes and effects of co-doping. (Zhang et al, 2016). Co-doping serves as a critical technique for enhancing doping characteristics in semiconductors, with the potential to decrease defect formation energy by leveraging Coulomb interaction or covalent coupling among co-dopants. This method also aids in reducing the transition energy level through level repulsions. Nonetheless, the success of co-doping is contingent upon the specific types of co-dopants employed, as there are instances where negative consequences may arise. (Dou et al, 2021).

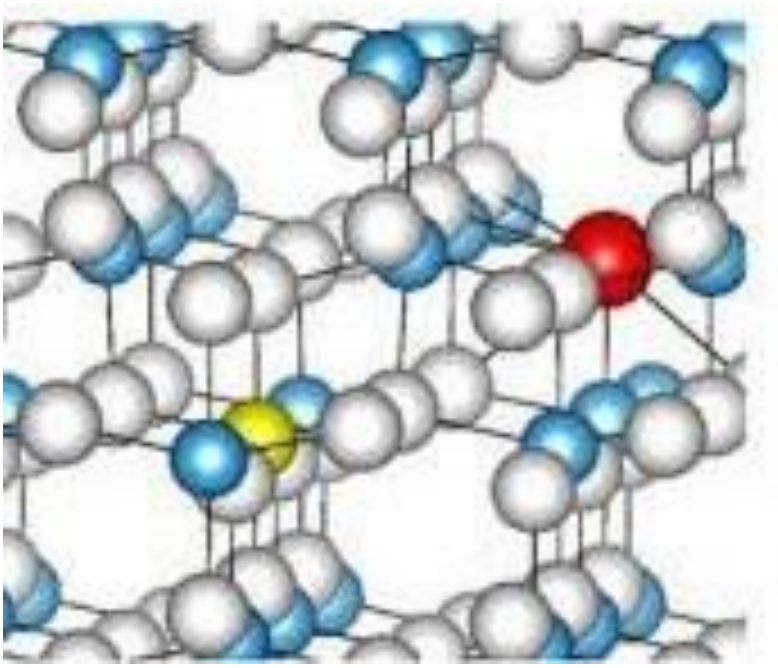

Figure 2.4: Co-Dopant nanoparticle

2.2.2 Synthesizing Nanoparticles

A nanoparticle is typically described as a particle ranging in size from 1 to 100 nanometers. Various terms have been utilized to characterize nano-scale drug delivery systems. Typically, polymers or lipids are employed as carriers for the drug, with the particle sizes spanning from a few nanometers to a few hundred nanometers.

To enhance nanoparticles as drug carriers, researchers have explored novel polymers and innovative approaches to advance drug delivery systems (Pal et al, 2011). These methods are broadly categorized into two approaches: top-down and bottom-up techniques.

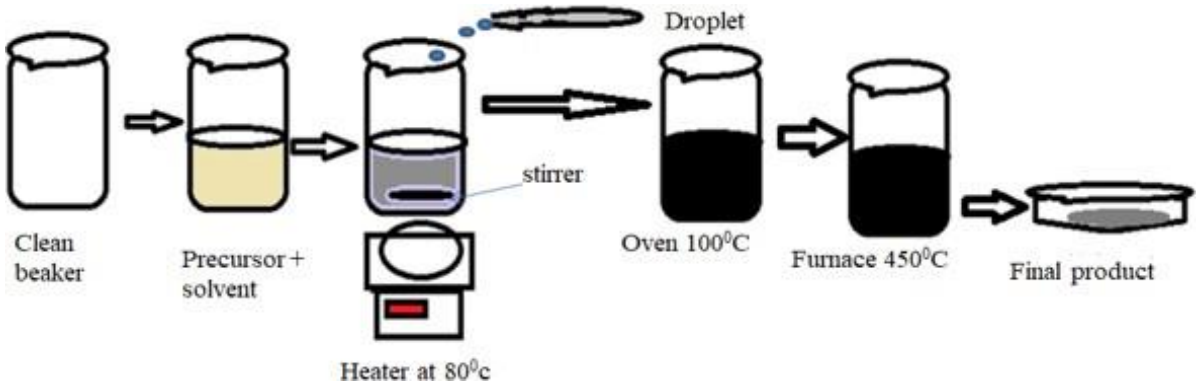

Figure 2.5: Synthetizing nanoparticle

2.2.3 Sol-Gel Method

The sol-gel synthesis method, which involves the hydrolysis and condensation of molecular precursors, is widely employed to produce a diverse range of inorganic materials. This technique is notably advantageous for generating both inorganic and organic-inorganic hybrid polymers. One key benefit of the sol-gel approach is the ability to conduct the entire process under gentle conditions.

Unlike solid-state processes, sol-gel methods offer the unique opportunity to manipulate reaction pathways at a molecular level while transitioning from precursor species to the final product. Consequently, sol-gel processes facilitate the creation of nanoparticles with precisely defined and uniform crystal structures, as well as exceptional purity and consistency. Sol-gel chemistry is intricate due to various factors, including the high reactivity of metal oxide precursors with water, the dual role of water as both a ligand and a solvent, and the necessity to rigorously control multiple reaction parameters (such as hydrolysis and condensation rates, pH, temperature, mixing methods, oxidation rate, etc.) to ensure the reproducibility and reliability of the synthesis procedure.

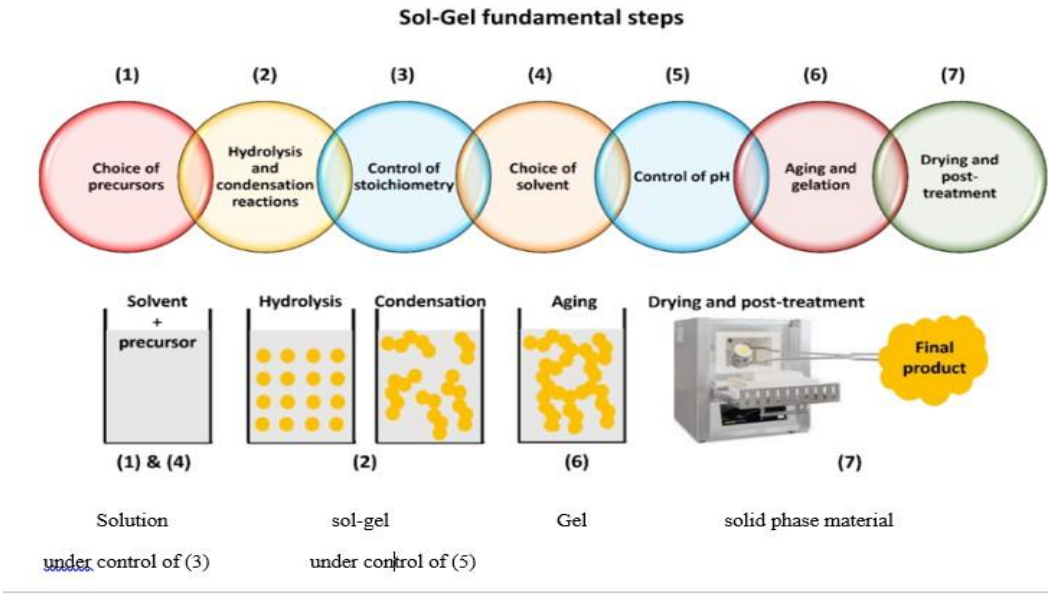

Figure 2.6: sketch of sol-gel

2.3 Sol-Gel Basic Strategies

The Sol-Gel process encompasses fundamental strategies crucial for the successful synthesis of materials. These strategies focus on manipulating precursor chemistry, reaction conditions, and post-treatment processes to regulate the development of desired materials. Below are the key basic strategies integral to the Sol-Gel process:

Precursors: The initial stage in the Sol-Gel process involves selecting suitable precursors. Metal alkoxides are commonly preferred due to their high reactivity and solubility in organic solvents, while metal chlorides are also utilized. The choice of precursors significantly impacts the composition and characteristics of the resulting material. Nucleophilic reactions play a central role in Sol-Gel chemistry, influencing the reactivity of metal alkoxides.

The reactivity levels are predominantly influenced by factors such as the metal atom's electronegativity, coordination number, and the steric hindrance from alkoxide groups. For instance, silicon alkoxides demonstrate relatively low reactivity, often requiring acid or base catalysis, or nucleophiles' activation to enhance hydrolysis and condensation rates. Conversely, transition metal alkoxides tend to be highly reactive, necessitating stabilization measures to prevent rapid condensation (Lebeau and S. et al, 1999).

Hydrolysis and condensation reactions: The Sol-Gel process consists of two primary reactions: hydrolysis and condensation. In the hydrolysis step, the metal alkoxide precursor interacts with water or hydroxide ions, resulting in the production of metal hydroxides or metal oxides. Following hydrolysis, the hydrolyzed species proceed to the condensation phase, where they engage in reactions with one another to establish metal-oxygen-metal bonds. This process ultimately leads to the creation of a three-dimensional network structure.

Controlled stoichiometry: Ensuring precise control over the stoichiometry of the precursor components is essential to attain the intended composition of the ultimate material. To achieve this, meticulous adjustment of the molar ratios of water, alcohol (solvent), and metal alkoxide is necessary. This control is vital for regulating the hydrolysis and condensation reactions effectively while also preventing any unintended side reactions from occurring.

Solvent choice: The selection of solvent plays a vital role as it impacts the solubility of the precursors, the speed of hydrolysis and condensation reactions, and the stability of the sol. Typical solvents used include alcohols such as methanol, ethanol, isopropanol, and water. It is crucial for the solvent to be compatible with the precursors and facilitate the creation of uniform sol dispersion.

PH control: The pH level of the Sol-Gel system is crucial in deciding how much hydrolysis and condensation reactions occur. By setting the pH within a particular range, it can enhance the creation of the intended material and avoid the formation of undesired phases.

Aging and gelation: Allowing the sol to age for a period helps in promoting further condensation reactions and rearrangement of the structure, resulting in the creation of a solid gel network. This aging period enables the colloidal solution to mature and settle, encouraging the formation of stronger metal-oxygen-metal connections within the material. With ongoing aging, the gel structure becomes more defined, ultimately reaching the crucial stage of gelation.

Gelation signifies the change of the 'sol' from a liquid colloidal state to a solid gel with a consistent three-dimensional structure. During this critical phase, the gel effectively traps the liquid phase within its framework, obtaining the unique properties and structure of the ultimate material.

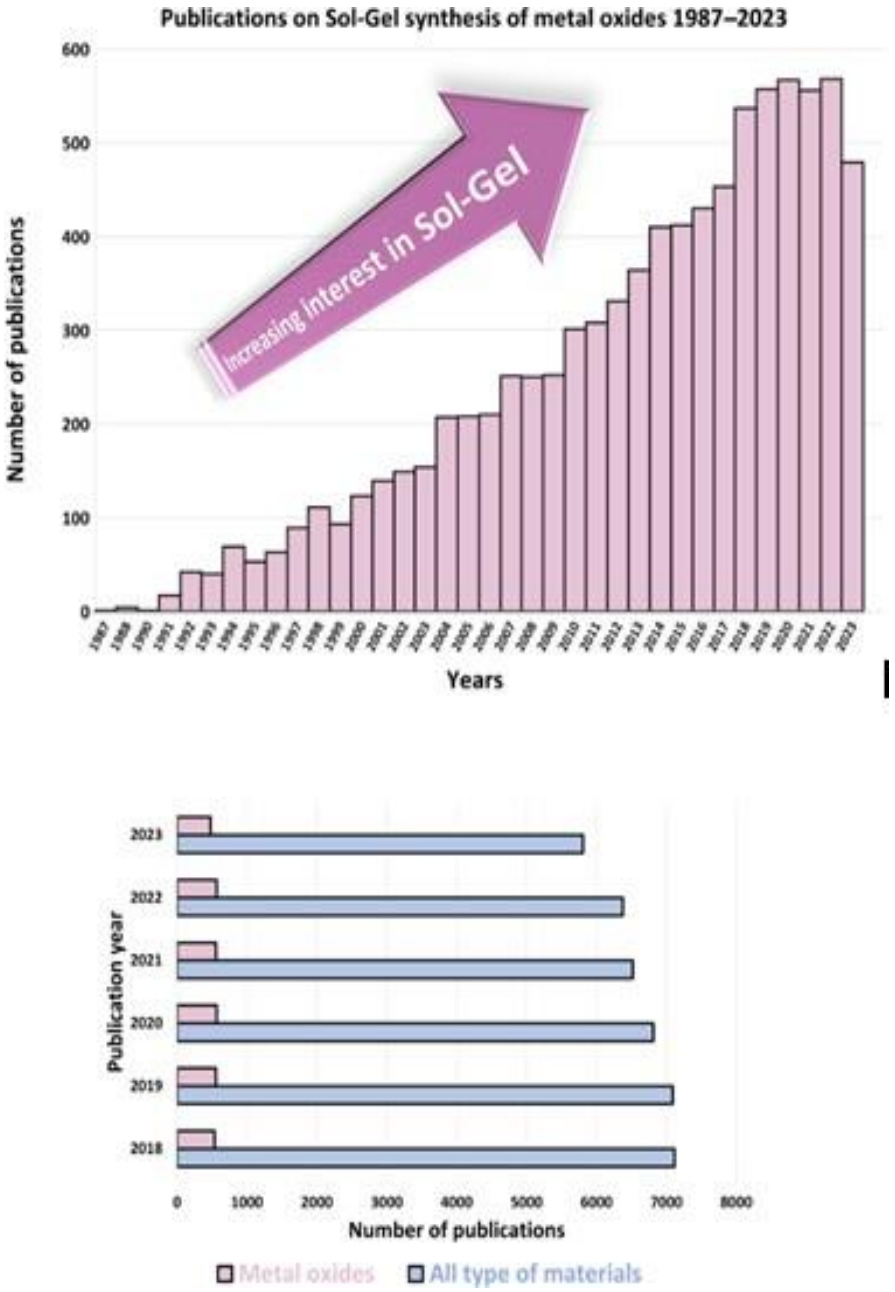

Figure 2.7: Number of publications on Sol-Gel synthesis of metal oxides (1987–2023)(Rex and Dos Santos, 2023) (Top) and its comparison with synthesis of other materials for the last five years (Bottom), from Web of Science using the search words ‘Sol-Gel’ and ‘metal oxides’, 31 January 2024.

Drying and post-treatment: After separating the phases of the gel through centrifugation, the gel is usually dried to eliminate the solvent and create a porous solid. Based on the intended use and requirements, additional steps like calcination/sintering or modifying the surface may be performed to improve the properties of the end product.

Through meticulous control of these essential procedures, scientists can customize the composition, structure, and characteristics of the materials produced using the Sol-Gel method, rendering it a versatile and extensively utilized approach in materials synthesis. Figure 2.7 illustrates the growing enthusiasm in recent years for the Sol-Gel technique for fabricating metal oxide materials

2.4 Synthesis Approaches

2.4.1 Top-down approach

The top-down approach starts with macroscopic structures and involves processes that break them down into nanoparticles. These methods require substantial installations and significant capital investment for setup, making them expensive and unsuitable for mass production. They are more suitable for laboratory experiments due to their costly nature. This approach relies on material grinding and is not suitable for handling soft samples. Figure 2.8 provides a visual representation of this method.

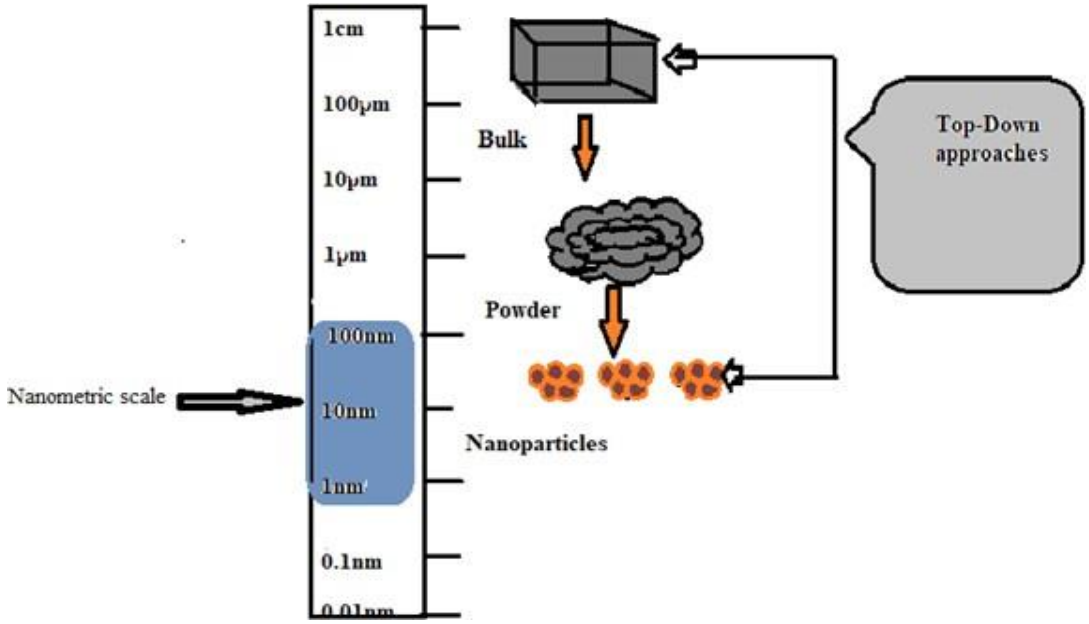

Figure 2.8: Top-down approach

2.4.2 Bottom-up approach

Bottom-up approaches for producing Nano-materials involve reducing the size of material components to the atomic level, followed by additional processes that result in the formation of nanostructures. As the process continues, the forces at the Nano scale bring together basic units to form larger, stable structures. This method primarily relies on the concept of molecular recognition (self-assembly), where components naturally assemble into larger structures. Many of these techniques are still in the developmental stage or are just starting to be employed for the industrial production of nanoparticles. Figure 2.9 provides a visual representation of this approach (Pati et al 2021).

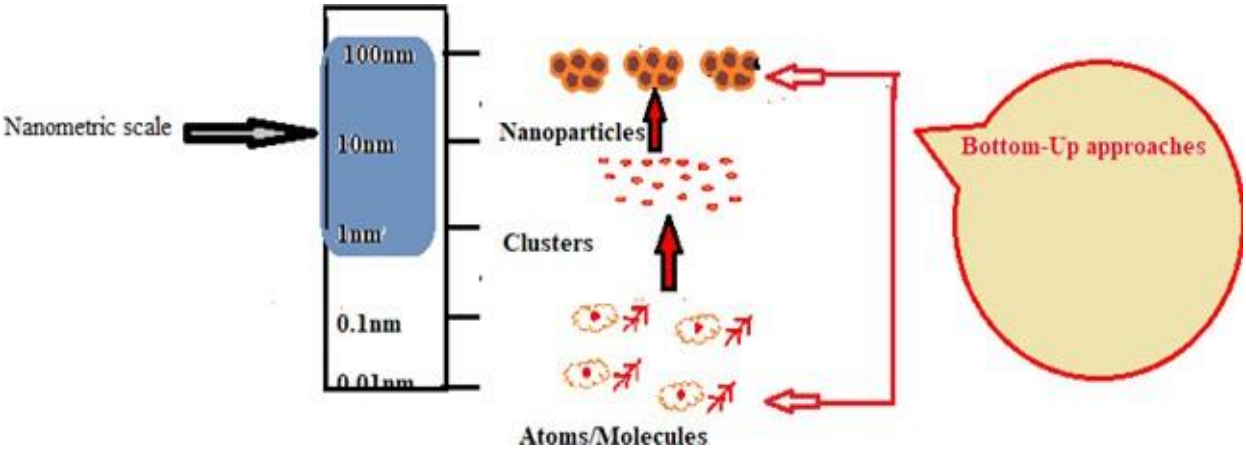

Figure 2.9: Bottom-up approach

2.5 Characterization Nanoparticles

The key factors examined during the characterization of nanoparticles include their size and shape. Additionally, we can analyze aspects such as size distribution, extent of aggregation, surface charge, surface area, and to some extent, assess the surface chemistry. The size, distribution, and organic ligands on the particle surfaces can impact other properties and potential applications of the nanoparticles. Furthermore, the crystal structure and chemical composition of the nanoparticles are extensively studied as an initial step following their synthesis. (Cuenya et al, 2010). Up to this point, there haven't been any established protocols for this purpose. Reliable and robust measurement techniques for nanoparticles will significantly influence the adoption of these materials in commercial applications and enable the industry to adhere to regulations (Committee et al., 2021). However, there are significant challenges in analyzing nano-materials due to the interdisciplinary nature of the field, the lack of appropriate reference materials for calibrating analytical tools, the complexities associated with sample preparation for analysis, and the interpretation of the data.

2.5.1 X-ray powder diffraction (XRD)

X-ray powder diffraction (XRD) is a quick analytical method mainly employed for identifying the phases of a crystalline material and can offer details on unit cell dimensions (Ali et al., 2022). The material being examined is finely ground, mixed uniformly, and the overall composition is established.

2.5.2 UV-Vis Spectroscopy (or Spectrophotometry)

UV-Vis Spectroscopy (or Spectrophotometry) is a quantitative method utilized to determine the light absorption of a chemical substance (Rocha et al., 2018). This is achieved by assessing the light intensity passing through a sample in comparison to the intensity of light passing through a reference sample or blank.

2.5.3 PL (Photoluminescence Spectroscopy)

PL (Photoluminescence Spectroscopy) utilizes a laser beam to capture the light emitted by a substance as it transitions from the excited state to the ground state upon laser excitation (Gfroerer et al., 2000). Through analyzing the luminescence spectrum, one can detect material defects and impurities.

2.5.4 Scanning electron microscopy (SEM)

Scanning electron microscopy (SEM) is extensively utilized for studying EVs and offers details on size and morphology. SEM operates by using a focused electron beam to scan the sample, interacting with atoms in the sample to generate three-dimensional surface topography (Uchic et al., 2007).

2.5.5 Transmission Electron Microscopy (TEM)

Transmission Electron Microscopy (TEM) is a method for imaging the internal structure of solids by transmitting a beam of high-energy electrons through the material (Thomas and M. et al, 2004). This setup can be likened to a conventional optical microscope with transmitted illumination, also known as a biological microscope (Zuo and S. et al, 2017).

Chapter 3

Methodology

In this thesis work experimental method and steps are:-Study and hypothesize the experimental Procedure, prepare suitable working area, collecting the necessary material and chemical, select synthesizing approach, take the measurement according to the theoretical calculation, apply sol-gel formation steps, characterizing the nanoparticle using XRD, PL, and SEM, and analyzing the data using Origin19.

3.1 Materials and chemicals

The materials and chemicals required for doping and co-doping of Pbs, CuPbS, FePbS, and co-doping of CuPbS with FePbS include beakers, graduated cylinders, digital electronic analytical balances, spoons, a heater, pH meter, thermometer, centrifuge, drying oven, furnace, test tubes, droppers, and ceramic crucible cups. As for the chemicals and solvents needed for the synthesis process, they consist of lead chloride, thiourea, ammonia, copper sulfate, iron sulfate, distilled water, deionized water, and ethanol alcohol.

3.2 Methods

Initially, conducting a survey on the fundamental properties of semiconductors; Once familiar with the common properties of semiconducting chemicals, using thin chloride as a precursor. The experiment proceeds well, but to uncover new findings regarding a nano powder, we utilize lead as the precursor and examine the properties of this chemical; Following the procedure for preparing lead sulfide from lead chloride using a sol-gel method to obtain a nano-powder, and further doping with copper and iron, then co-doping CuPbS and FePbS to create selective and active semiconducting

material characterizing the nanoparticles using SEM, PL, and XRD. This aims to understand the properties of optoelectronic semiconducting materials. Safety equipment for the experiment includes a mask, gloves, cleaning soap, brush, and soft surfaces to work on.

Experiment

In this experimental method, we will utilize various chemicals to synthesize lead sulfide (PbS) and dope it through chemical precipitation sol-gel processes. The chemicals involved are $PbCl_2$ as a precursor of lead, Thiourea (H_2N-CS-NH_2), Ammonia (NH_3OH), $CuSO_4 \cdot 5H_2O$, and $FeSO_4 \cdot 7H_2O$ solutions. The process includes stirring the mixture without heat, then heating it to 80 degrees Celsius for 2 hours, followed by allowing the solution to settle overnight. The chemical solutions are washed using centrifugation for 10 minutes, four times with deionized water, twice with ethanol, and finally rinsed once more with deionized water. The collected samples are placed in a beaker and dried in an oven at 100 degrees Celsius for 24 hours. Additionally, a furnace set to 450 degrees Celsius is used for 2 hours. Each step of the procedure will be meticulously followed. The properties of the synthesized nanoparticles will be examined using X-ray Diffraction (XRD), Scanning Electron Microscopy (SEM), and Photoluminescence (PL).

Preparation of PbS

To prepare a 100 cc solution of Lead Chloride ($PbCl_2$) with a concentration of 0.25M, the following calculation can be used: To calculate the amount of $PbCl_2$; Molarity (M) = moles of solute per liters of solution, Moles of $PbCl_2$ = Molarity x Volume (in liters), Moles of $PbCl_2$ = 0.25 mol/L x 0.1 L (since 100 cc = 0.1 L) and moles of $PbCl_2$ = 0.025 moles

To determine the molar mass of $PbCl_2$ (Lead Chloride): $PbCl_2$: Pb (Lead) = 207.2 g/mol, Cl (Chlorine) = 35.45 g/mol, molar mass of $PbCl_2$ = 207.2 g/mol (Pb) + 2(35.45 g/mol) (Cl) = 278.1 g/mol and calculate the mass of $PbCl_2$, mass of $PbCl_2$ = moles of $PbCl_2$ x molar mass of $PbCl_2$= 0.025 moles x 278.1 g/mol= 6.813 grams

Therefore, to prepare a 100 cc solution of Lead Chloride with a concentration of 0.25M, you would need approximately 6.813 grams of $PbCl_2$.

Procedure

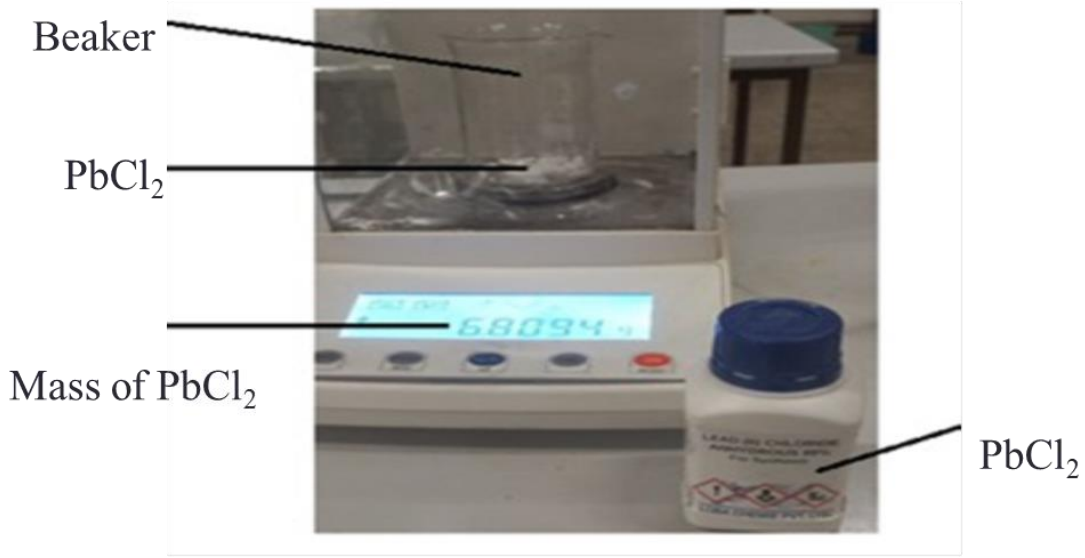

Figure 3.1: Measurement of $PbCl_2$

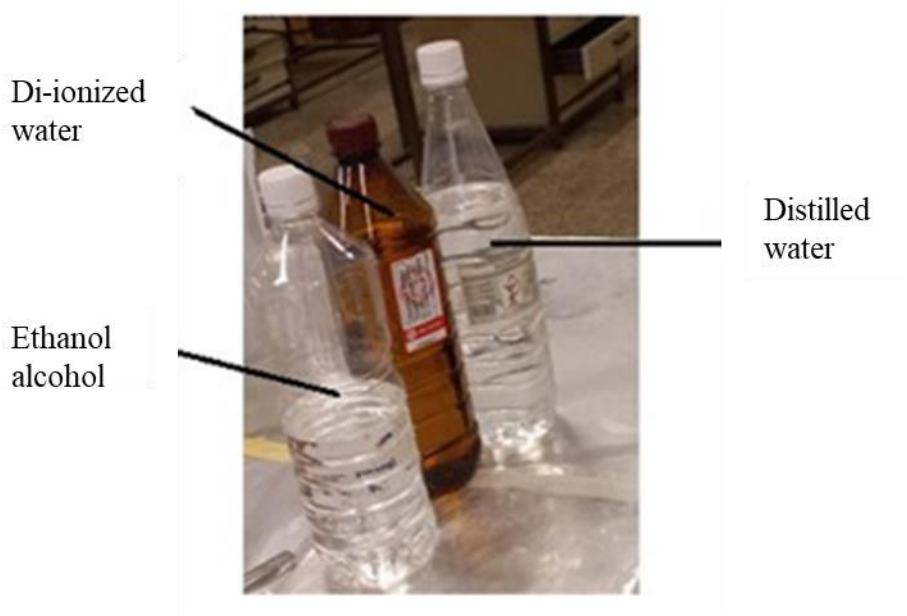

Figure 3.2: Solvent and ethanol alcoho

To prepare a H_2N-CS-NH_2 solution with a concentration of 0.25 mol, you would need to calculate the molecular weight of thiourea (H_2N-CS-NH_2): the atomic masses are: H = 1, C = 12, N = 14, S = 32, O = 16, molecular weight of thiourea = 2(1) + 12 + 14 + 32 + 2(1) = 76 g/mol and to determine the mass of thiourea needed: Mass (g) = Concentration (mol/L) * Volume (L) * Molecular weight (g/mol) Mass (g) = 0.25 mol/L * 0.1 L * 76 g/mol*0.98 = 4.6623 grams of thiourea

Therefore, to prepare a H_2N-CS-NH_2 solution with a concentration of 0.25 mol/L using 100 mL of solvent, you would need to dissolve 4.6623 grams of H_2N-CS-NH_2 in the solvent.

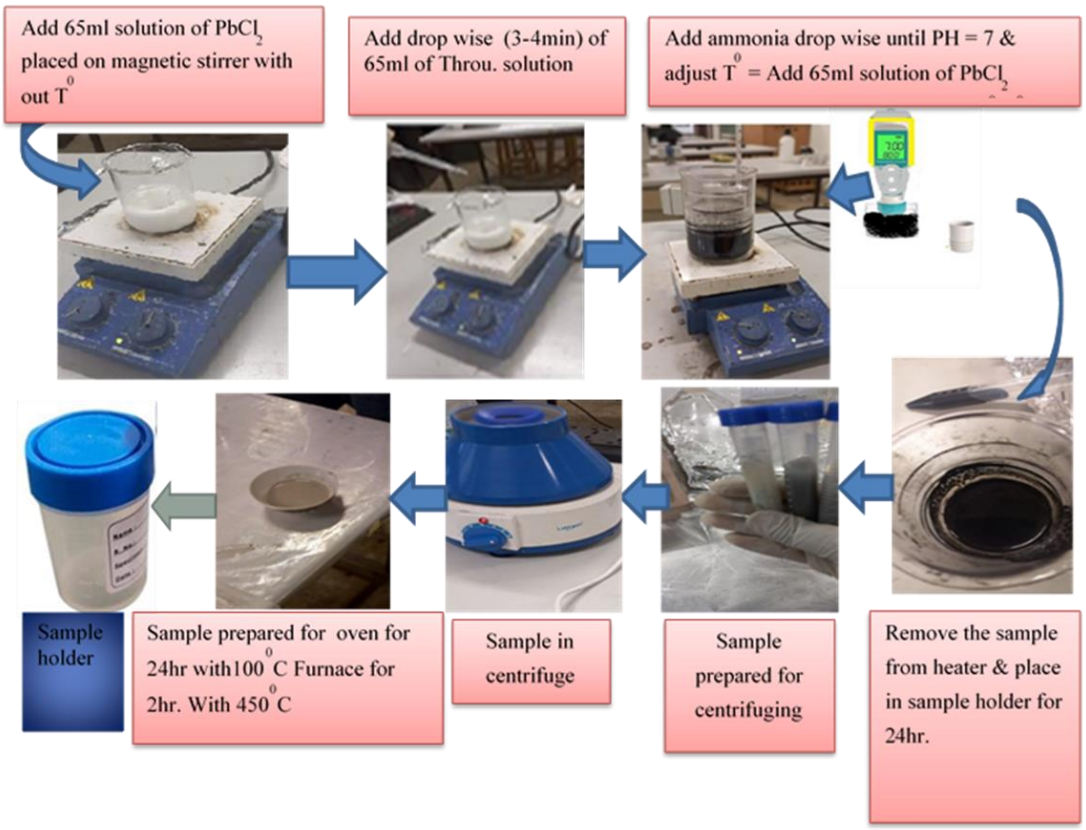

Figure 3.3: preparation of PbS nanoparticle

To synthesize lead sulfide (PbS) nanoparticles using the sol-gel method, follow this simplified procedure: Prepare 65 ml of lead sulfide (PbS) solution and 65 ml of thiourea (H2N-CS-NH2) solution in a beaker with a magnetic stirrer. Mix the solutions while adding ammonia dropwise to control and maintain the solution's pH value at 7 on the pH scale. Adjust the temperature to 80 degrees Celsius and allow the mixture to react for 2 hours. After the reaction, place the sample in a cold, clean, and dry place overnight for further processing. Wash the sample with deionized water using a centrifuge four times, followed by washing it with ethanol alcohol two times, and then once more with deionized water for 10 minutes each time. Collect the gel obtained from washing and place it in an oven for 24 hours at a temperature of 100 degrees Celsius. Increase the temperature to 450 degrees Celsius using a furnace for 2 hours to further heat the sample. Once the sample cools down, grind it and collect it in a clean, dry sample holder for further analysis or use.

Following these steps will help you synthesize lead sulfide nanoparticles using the sol-gel method effectively.

Preparation of doped CuPbS

To synthesize copper (Cu) doped with PbS nanoparticles using the sol-gel method and to prepare copper sulfate pentahydrate ($CUSO_4 \cdot 5H_2O$) with a mass of 1.03 grams, by calculating the molecular weight of copper sulfate pentahydrate ($CuSO_4 \cdot 5H_2O$): The atomic masses are: Cu = 63.5, S = 32, O = 16, H = 1, molecular weight of $CuSO_4 \cdot 5H_2O$ = 0.25 * 277.9 * 0.995 * 15 / 1000 = 1.03 grams.

Therefore, to synthesize copper doped with lead sulfide nanoparticles via the sol-gel method and prepare 1.03 grams of copper sulfate pentahydrate.

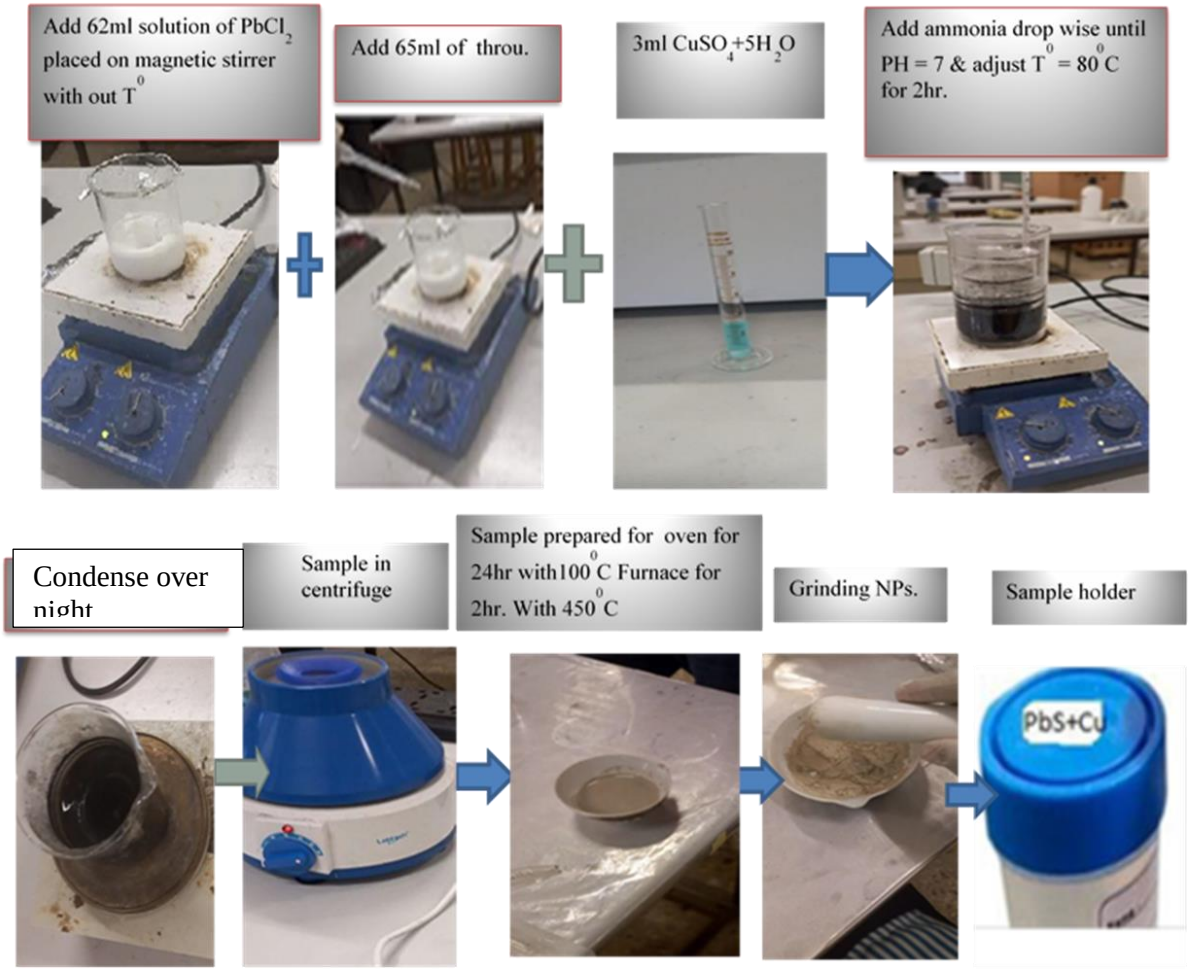

Figure 3.4: preparation of CuPbS nanoparticle

To synthesize doped copper lead sulfide (CuPbS) nanoparticles using the sol-gel method, follow this simplified procedure: Prepare 62 ml of lead sulfide (PbS) solution and 65 ml of thiourea (H_2N-CS-NH_2) solution in a beaker with a magnetic stirrer. Mix the solutions while adding ammonia drop wise to control and maintain the solution's pH value at 7 on the PH scale and drop wise 3ml of $CuSO_4$+$5H_2O$ in the solution. Adjust the temperature to 80 degrees Celsius and allow the mixture to react for 2 hours. After the reaction, place the sample in a cold, clean, and dry place overnight for further processing. Wash the sample with deionized water using a centrifuge four times, followed by washing it with ethanol alcohol two times, and then once more with deionized water for 10 minutes each time. Collect the gel obtained from washing and place it in an oven for 24 hours at a temperature of 100 degrees Celsius. Increase the temperature to 450 degrees Celsius using a furnace for 2 hours to further heat the sample. Once the sample cools down, grind it and collect it in a clean, dry sample holder for further analysis.

Preparation of dopes $FeSO_4.7H_2O$ with PbS

To synthesize iron doped with lead sulfide nanoparticles using the sol-gel method and prepare a 0.25 M (molar) solution of iron (II) sulfate heptahydrate ($FeSO_4 \cdot 7H_2O$). Mass in gm = concentration M *molar mass (g/mol)*volume (L) the concentration of sample 0.25 M, molar mass of $FeSO_4 \cdot 7H_2O$ = 277.9 g/mol and volume = 0.995 L (assuming this is the volume specified for the solution), Factor for mass calculation = 15 / 1000. mass g = 0.25 * 277.9 *0.995 * 15/1000 calculating the mass is equal to 1.03 g. Therefore, to synthesize iron doped with lead sulfide nanoparticles by the sol-gel method and prepare a 0.25 M solution of iron(II) sulfate heptahydrate, you would need approximately 1.03 grams of $FeSO_4 \cdot 7H_2O$ dissolved in 0.995 liters of solvent. Form solution of lead chloride, H_2N-CS-NH_2 and iron; add 62ml $PbCl_2$ to beaker and stir without temperature, adding 65ml H_2N-CS-NH_2 and drop ammonia until PH = 7 add 3ml iron 5 percent of iron the solution adjust temperature 80 degree centigrade and wait for 2hr. Wash the sample by centrifuge using distilled water 4 times in 10 min. and 2 times by ethanol in 10 min; again wash by distilled water once again in 10 min. Applying the same procedure and the collect dry sample in to sample holder.

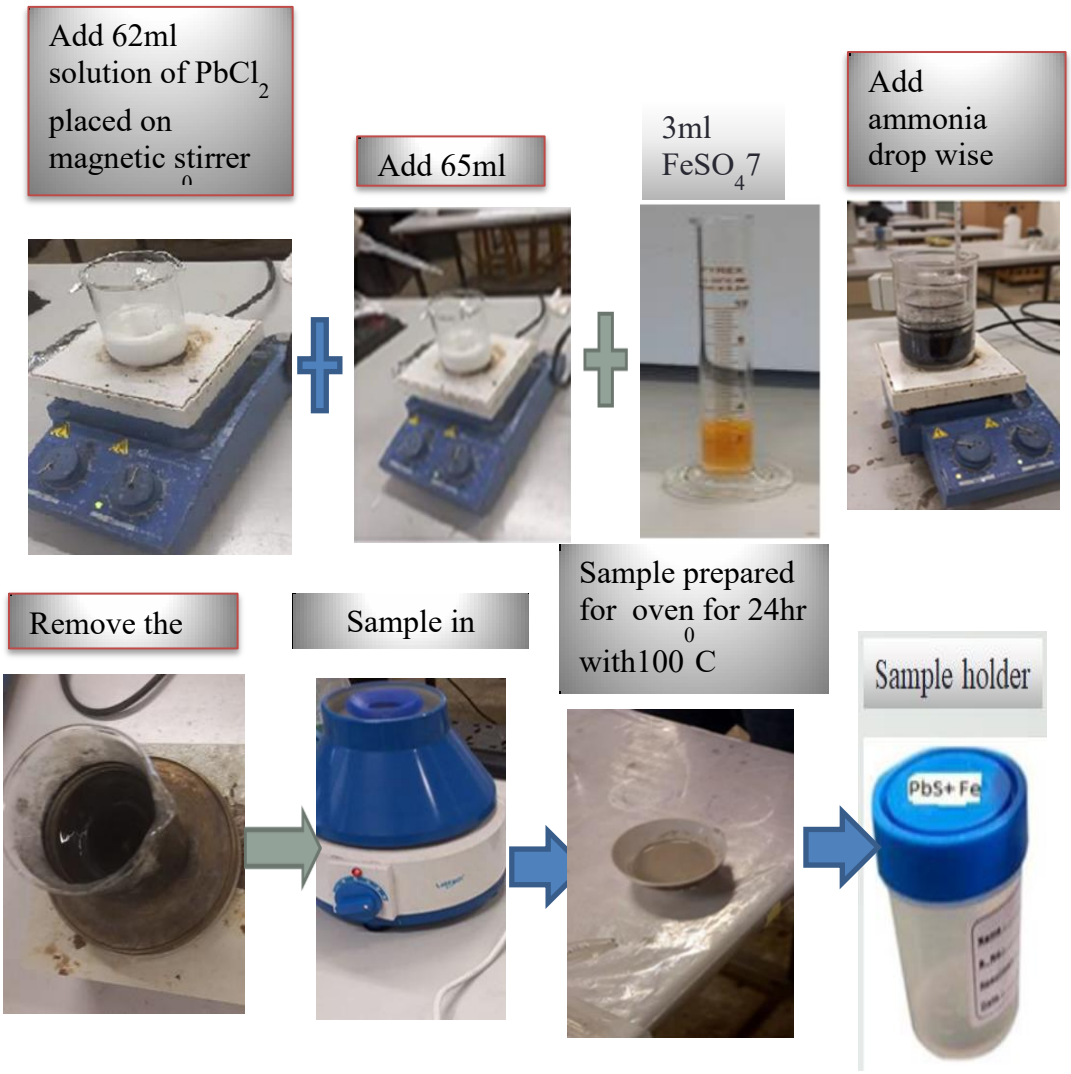

Figure 3.5: preparation of FePbS nanoparticle

Preparation of Co-doped CuFePbS

To synthesis Iron and copper co-doped with PbS nanoparticles by sol- gel method.

Mass of $PbCl_2$ = 6.813 grams and mass of $H_2N\text{-}CS\text{-}NH_2$ = 4.665grams.

To prepare $FeSO_4.7H_2O$ mass (gm) = 0.25 x 277.9 x 0.995 x 15/1000 = 1.03gm and

to prepare $CuSO_4.5H_2O$ mass (gm)=0.25 x 249.69 x 0.995 x 15/1000 = 0.931gm.

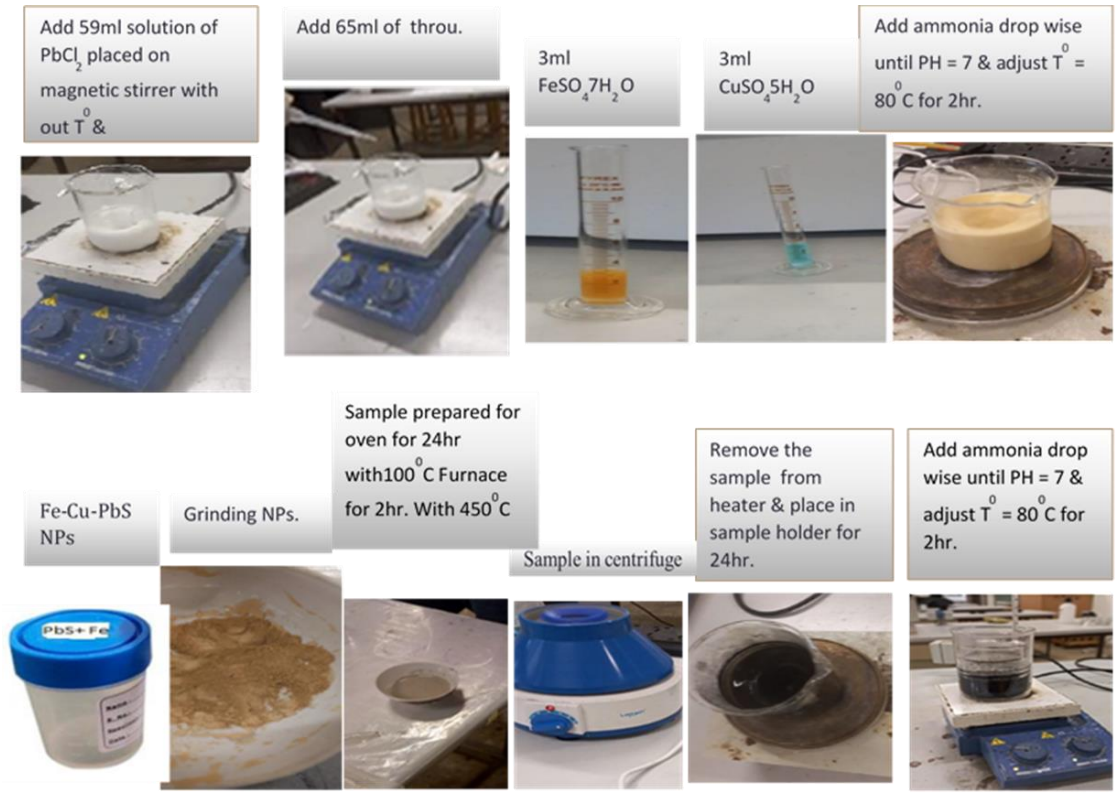

Figure 3.6 : preparation of Co-dopant nanoparticle.

To simplify the instructions provided for preparing a solution containing lead chloride, thiourea, copper, and iron, you would follow these steps:- In a beaker, add 59 ml of lead chloride solution and stir without changing the temperature. Add 65 ml of thiourea solution while slowly adding ammonia until the pH reaches 7. Introduce 3 ml of a 5% copper solution and 3 ml of a 5% iron solution into the mixture within 2 minutes. Adjust the temperature to 80 degrees. Celsius and allow the solution to react for 2 hours. Wash the sample by transferring it to a centrifuge and rinsing it with distilled water four times for 10 minutes each time.

Subsequently, rinse the sample with ethanol twice for 10 minutes each. Complete the washing process by rinsing the sample with distilled water once more for 10 minutes. Repeat the entire procedure as needed and then collect the dried sample in a sample holder for further use. Following these simplified steps will help you create the desired solution containing lead chloride, thiourea, ammonia, copper, and iron effectively.

Chapter 4

Result and Discussion

In order to evaluate the crystal structure, absorption properties, and optical band-gap of the synthesized nanoparticles, various analytical techniques including X-ray diffraction (XRD), scanning electron microscopy (SEM), and photoluminescence (PL) were utilized.

For the investigation of the quality of the prepared nanoparticles, the laboratory employed the sol-gel method to synthesize and characterize the doping and co-doping of copper (Cu), iron (Fe), and lead sulfide (PbS).

The analysis of the nanoparticle samples was conducted using X-ray diffraction (XRD), photoluminescence (PL), and scanning electron microscopy (SEM) equipment. The XRD machine produced results that indicated a three-dimensional periodic pattern, signifying a crystalline structure. The shape and width of peaks observed in the XRD data provide insights into the crystallinity of the material. Sharp, narrow peaks indicate high crystallinity, while broader peaks suggest an amorphous or less crystalline structure.

The X-ray diffraction pattern from the synthesized nanoparticles was consistent with a cubic structure of PbS, with sharp and intense diffraction peaks indicating good crystallinity and peak broadening suggesting nanoparticle formation. The material was classified as a semiconductor based on its interaction with light, corresponding to a bandgap that absorbs or emits light in the near ultraviolet to visible range. These properties make it suitable for applications in optoelectronics and semiconductor devices.

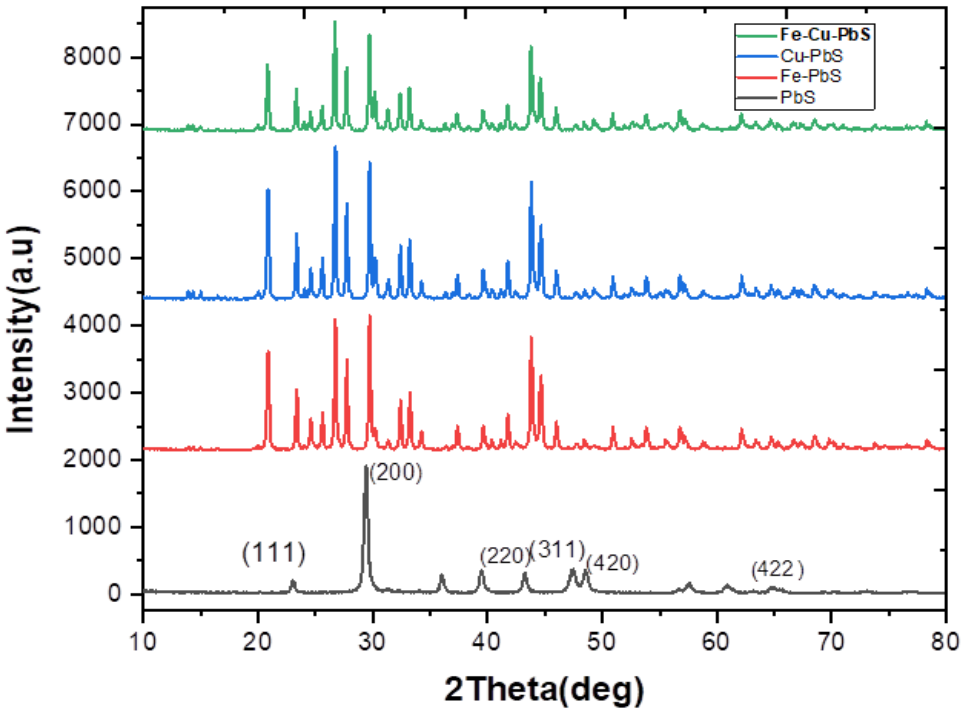

Figure 4.1: XRD Reading of PbS, FePbS, CuPbS and CuFePbS nanoparticle.

Sample	2θ	Dopant	hkl	FWHM	Crystal Size (nm)	Dislocation (δ) = $1/D^2$
FePbS	29.75	5%	200	0.1767	48.61	0.00042
PbS	29.417	0%	200	0.3794	22.62	0.00192
CuFePbS	26.755	10%	111	0.1872	45.58	0.00048
CuPbS	26.72	5%	111	0.1913	44.67	0.000502

Table 4.1: XRD maximum peak reading with Crystal size

The analysis of the nanoparticles reveals narrow peak widths, indicating large crystal sizes and strong peaks suggestive of crystallographic planes or potential phases within the nanoparticles. By comparing the positions and intensities of these peaks with data from the JCPDS (Joint Committee on Powder Diffraction Standards) database, it is possible to identify the phases present in the nanoparticles. The distinct peaks observed in the XRD pattern indicate the absence of amorphous content in the nanoparticles.

The crystalline size of the nanoparticles was calculated to be approximately 48.61

nm, 22.62 nm, 45.58 nm, and 44.67 nm using the Scherrer equation and the Full Width at Half Maximum (FWHM) of the diffraction peaks corresponding to (200), (200), (111), and (111) planes, respectively. All these diffraction peaks align with the pure cubic phase of lead sulfide (PbS) (JCPDS card No. 05-0592), with the peaks originating from the (111), (200), (220), and (420) planes, respectively.

The highest peak intensity indicates that the grains are preferentially oriented along the (200) direction, while the broad diffraction peaks (FWHM) suggest the formation of nanoparticles with reduced sizes.

Crysatal Size D = $\frac{K\lambda}{\beta_{hkl}\cos_{hkl}}$

Where

β_{hkl} = half width of diffraction band

K = 0.95 – 0.98 (Shape factor)

θ_{hkl} = Bragg – Diffraction angle

The decrease in dislocation density was observed with an increase in crystal size. This decrease could be attributed to a reduction in the presence of grain boundaries, which often occurs as the crystal size of the particle increases. Furthermore, the Full Width at Half Maximum (FWHM) of the peaks decreased with the increase in the thickness of the doped and co-doped lead sulfide (PbS) nanoparticles. This trend confirms an inverse relationship between dislocation density and crystallinity, suggesting that an increase in thickness enhances crystallinity.

As the thickness of the nanoparticles increased, there was a corresponding change in the crystallite size, resulting in decreased dislocation density and strain. Therefore, the findings indicate that an increase in thickness leads to improved crystallinity, as evidenced by the interplay between crystal size, dislocation density, and strain in the synthesized nanoparticles.

The dislocation density decreased with increasing crystal size. It may be due to a decrease in the occurrence of grain boundaries because of an increase in the crystal size of the particle. FWHM of the peaks decreased with increase in thicknesses of the doped and co-doped PbS nanoparticles, thus confirming inverse relation between dislocation density and crystaline, and hence it is concluded that increase in thickness improved crystallinity. As the thickness increased, the crystallite size changed, so dislocation density and strain decreases.

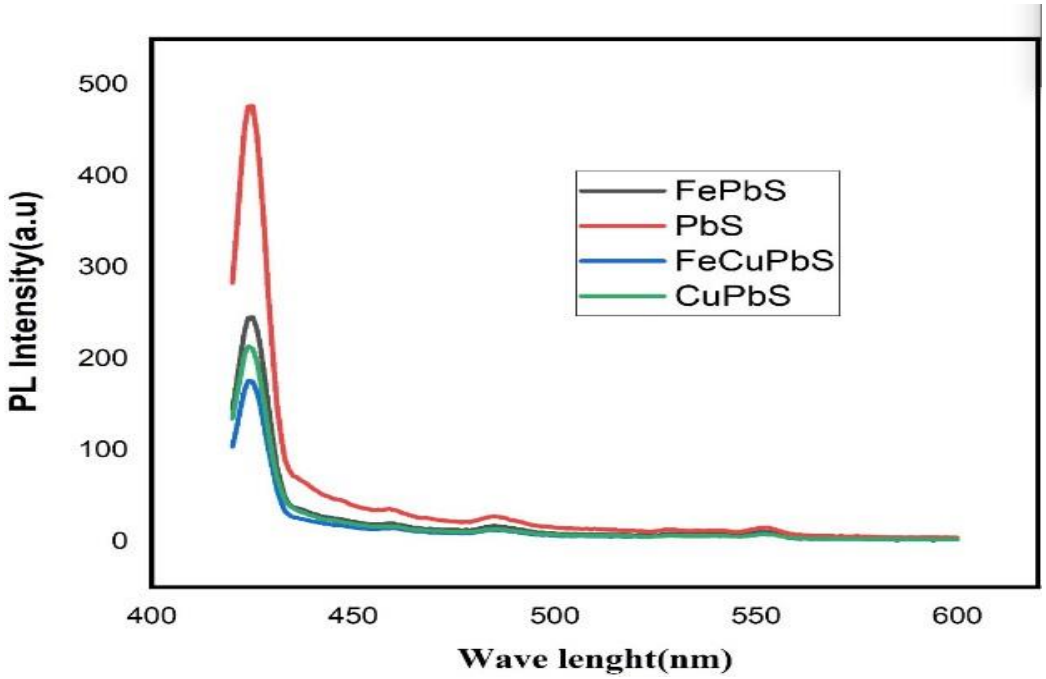

Figure 4.2: PL Reading of nanoparticle PbS, FePbS, CuPbS and CuFePbS.

The photoluminescence emissions at 405nm, 425nm, and 423nm, which may result from quantum confinement in the nanoparticles, indicate specific band gap energies for different materials. PbS demonstrates a band gap energy of 3.062eV, FePbS shows 2.931eV, CuPbS exhibits 2.931eV, and FeCuPbS displays 2.917eV, all leading to emissions at those particular wavelengths. These fluorescence properties have a wide range of applications, including bio-imaging, sensors, optoelectronic devices, and light-emitting devices.

Moreover, it is observed that the intensity of the peak decreases with increasing doping concentrations. For instance, PbS without any dopant exhibits a high peak intensity, whereas FeCuPbS with a considerable amount of dopant shows a

significantly lower peak intensity. This variation in intensity with different concentrations highlights the influence of dopants on the photo-luminescent properties of the materials.

The scanning electron microscope (SEM) images for nanoparticles of PbS, FePbS, CuPbS, and FeCuPbS are depicted in Fig. 4.3 (a - d). Upon observing the figures, it was noted that doping and co-doping resulted in changes in the surface morphology of PbS, revealing a densely packed crystalline structure. Fig. 4.3 (a) illustrates the surface of a pure PbS nanoparticle, showing nano-sized pyramidal grains with a porous texture covering the entire film surface. The grains tend to agglomerate, forming a cubic arrangement as evident in Fig. 4.3(b) due to a 5 percent doping of Copper and Iron.

Furthermore, as the level of Cu and Fe co-doping increases up to 10 percent the agglomeration of grains intensifies in Fig. 4.3 (d), reading to a reduction in pinholes that were visible in Fig. 3 (c) and 3 (d). This agglomeration induced by Cu, Fe doping, and co-doping also encourages grain growth. All the deposited films are composed of nano-sized grains distributed across the surface. The inherent structure of PbS, characterized by a large surface area is instrumental in the development of optoelectronic materials.

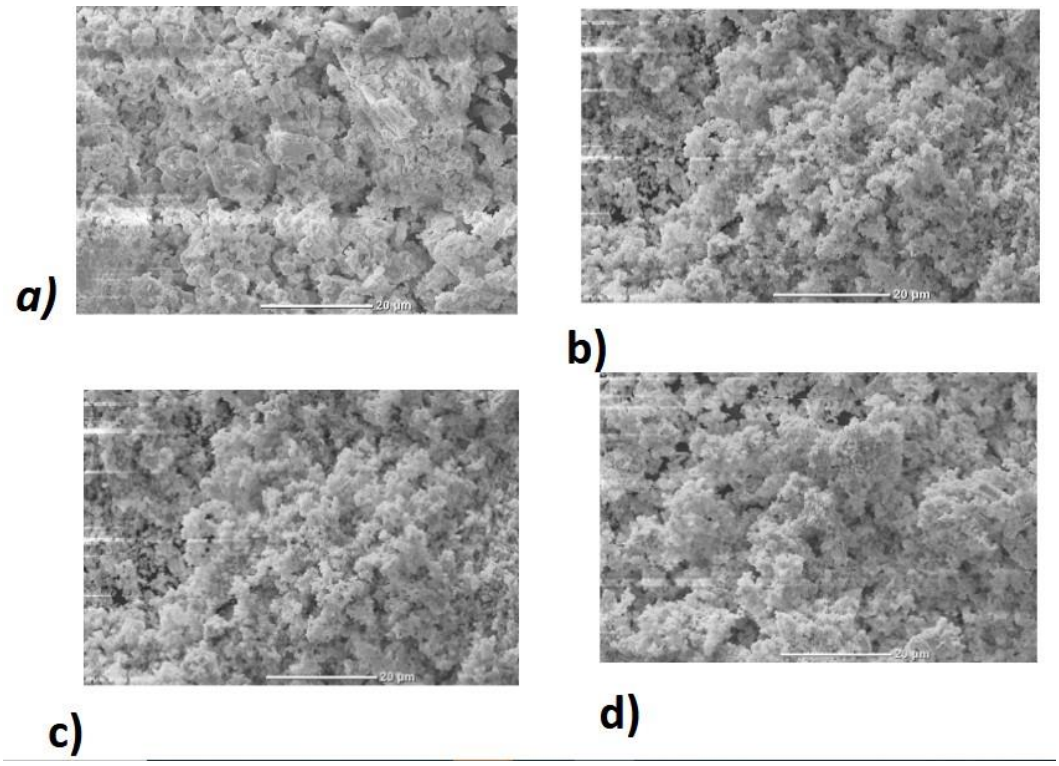

Figure 4.3: SEM Reading of nanoparticle PbS, FePbS, CuPbS and CuFePbS.

Conclusion and Recommendations

Synthesizing a nanoparticle method is simple and cost effective, easily handling, and high productive. the nanoparticle was characterized by different method XRD,PL. PL emission at 405 nm, 423 nm,423 nm, and 425 nm may find applications in areas such as biological imaging, fluorescent labeling, sensing technologies, display technologies, and quantum dot-based devices. The X-ray diffraction pattern of the as-synthesized nanoparticles were indexed with cubic structure of PbS. The sharp intense diffraction peaks indicating the good crystallinity and broadening of peak indicating the formation of nanoparticle. SEM micrographs for a nanoparticle of PbS, FePbS, CuPbS revealed the surface photograph image of pure PbS nanoparticle, it is clearly seen that the nano-sized pyramidal shaped grains with porous nature covered the entire film surface. There is agglomeration of grains which forms cubic nature and was noticed owing to doping of 5 percent of copper and iron. Further in Cu and Fe co-doping level up to 10 percent displays an increase in agglomeration level of the grains which reduces the pinholes. This agglomeration due to Cu, Fe doping and co-doping also promotes the grain growth. In another ways it shows its optical behavior, stability and performance of nanoparticles these can lead to advancement in developing nanomaterial.

Bibliography

Ali, A., Chiang, Y. W., and Santos, R. M. (2022). X-ray diffraction techniques for mineral characterization: A review for engineers of the fundamentals, applications, and research directions. *Minerals*, 12(2):205.

Chaves, A., Azadani, J. G., Alsalman, H., Da Costa, D., Frisenda, R., Chaves, A., Song, S. H., Kim, Y. D., He, D., Zhou, J., et al. (2020). Bandgap engineering of two-dimensional semiconductor materials. *npj 2D Materials and Applications*, 4(1):29.

Committee, E. S., More, S., Bampidis, V., Benford, D., Bragard, C., Halldorsson, T., Hernández-Jerez, A., Bennekou, S. H., Koutsoumanis, K., Lambré, C., et al. (2021). Guidance on technical requirements for regulated food and feed product applications to establish the presence of small particles including nanoparticles. *EFSA Journal*, 19(8):e06769.

Cuenya, B. R. (2010). Synthesis and catalytic properties of metal nanoparticles: Size, shape, support, composition, and oxidation state effects. *Thin Solid Films*, 518(12):3127–3150.

DeBenedictis, E. P., Badaroglu, M., Chen, A., Conte, T. M., and Gargini, P. (2017). Sustaining moore's law with 3d chips. *Computer*, 50(8):69–73.

Dou, B., Sun, Q., and Wei, S.-H. (2021). Optimization of doping cd te with group-v elements: A first-principles study. *Physical Review Applied*, 15(5):054045.

Enderlein, R. and Horing, N. J. (1997). *Fundamentals of semiconductor physics and devices*. World Scientific.

Gfroerer, T. H. et al. (2000). Photoluminescence in analysis of surfaces and interfaces. *Encyclopedia of analytical chemistry*, 67:3810.

Jaiswal, M. and Menon, R. (2006). Polymer electronic materials: a review of charge transport. *Polymer international*, 55(12):1371–1384.

Kato, T., Sasaki, H., Katagiri, T., Sasaki, H., Koiwai, K., Youki, H., Totsuka, S., and Ishii, T. (1991). The binding of basic fibroblast growth factor to alzheimer's neurofibrillary tangles and senile plaques. *Neuroscience letters*, 122(1):33–36.

Kim, K., Coh, S., Tan, L. Z., Regan, W., Yuk, J. M., Chatterjee, E., Crommie, M., Cohen, M. L., Louie, S. G., and Zettl, A. (2012). Raman spectroscopy study of rotated double-layer graphene: misorientation-angle dependence of electronic structure. *Physical review letters*, 108(24):246103.

Lebeau, B. and Sanchez, C. (1999). Sol-gel derived hybrid inorganic-organic nanocomposites for optics. *Current Opinion in Solid State and Materials Science*, 4(1):11–23.

Mott, N. (1972). Conduction in non-crystalline systems ix. the minimum metallic conductivity. *Philosophical Magazine*, 26(4):1015–1026.

Pal, S. L., Jana, U., Manna, P. K., Mohanta, G. P., and Manavalan, R. (2011). Nanoparticle: An overview of preparation and characterization. *Journal of applied pharmaceutical science*, (Issue):228–234.

Parveen, A., Agrawal, S., and Azam, A. (2018). Band gap tuning and fluorescence properties of lead sulfide pb0. 9a0. 1s (a: Fe, co, and ni) nanoparticles by transition metal doping. *Optical Materials*, 76:21–27.

Patil, N., Bhaskar, R., Vyavhare, V., Dhadge, R., Khaire, V., and Patil, Y. (2021). Overview on methods of synthesis of nanoparticles. *Int. J. Curr. Pharm. Res*, 13(2):11–16.

Patil, V. L. and Patil, V. L. (2021). Status of wireless air defence systems before word war ii. *Chronological Developments of Wireless Radio Systems before World War II*, pages 153–192.

Rex, A. and Dos Santos, J. (2023). The use of sol–gel processes in the development of supported catalysts. *Journal of Sol-Gel Science and Technology*, 105(1):30–49.

Riordan, M., Hoddeson, L., and Herring, C. (1999). The invention of the transistor. *Reviews of Modern Physics*, 71(2):S336.

Rocha, F. S., Gomes, A. J., Lunardi, C. N., Kaliaguine, S., and Patience, G. S. (2018). Experimental methods in chemical engineering: Ultraviolet visible spectroscopy—uv-vis. *The Canadian Journal of Chemical Engineering*, 96(12):2512–2517.

Rosario, S. R., Kulandaisamy, I., Arulanantham, A., Valanarasu, S., Hamdy, M. S., Al-Namshah, K., Alhanash, A. M., et al. (2019). Analysis of cu doping concentration on pbs thin films for the fabrication of solar cell using feasible nebulizer spray pyrolysis. *Materials Research Express*, 6(5):056201.

Satvekar, R., Tiwari, A., Rohiwal, S., Tiwale, B., and Pawar, S. (2015). A dna-assembled fe 3 o 4@ ag nanorod in silica matrix for cholesterol biosensing. *Journal of Materials Engineering and Performance*, 24:4691–4695.

Schubert, E. F. (2015). *Doping in III-V semiconductors*. E. Fred Schubert.

Teng, Y., Ren, Y., Sayed, M., Hu, X., Lei, C., Kumar, A., Hutchins, E., Mu, J., Deng, Z., Luo, C., et al. (2018). Plant-derived exosomal micrornas shape the gut microbiota. *Cell host & microbe*, 24(5):637–652.

Thomas, J. M. and Midgley, P. A. (2004). High-resolution transmission electron microscopy: the ultimate nanoanalytical technique. *Chemical communications*, (11):1253–1267.

Uchic, M. D., Holzer, L., Inkson, B. J., Principe, E. L., and Munroe, P. (2007). Three-dimensional microstructural characterization using focused ion beam tomography. *MRS bulletin*, 32(5):408–416.

Unno, Y. and Iwai, H. (1999). Future trends in large scale integrated circuit technologies from an industrial perspective. *Future trends in microelectronics*.

Wang, Y.-W. and Zheng, M.-Z. (2023). Characteristics and strategic significance of ic industry. In *Handbook of Integrated Circuit Industry*, pages 25–30. Springer.

Xu, Y. and Schoonen, M. A. (2000). The absolute energy positions of conduction and valence bands of selected semiconducting minerals. *American mineralogist*, 85(3-4):543–556.

Yoshida, M., Worlock, K. B., Huang, N., Lindeboom, R. G., Butler, C. R., Kumasaka, N., Dominguez Conde, C., Mamanova, L., Bolt, L., Richardson, L., et al. (2022). Local and systemic responses to sars-cov-2 infection in children and adults. *Nature*, 602(7896):321–327.

Zhang, J., Cheng, F., Li, J., Zhu, J.-J., and Lu, Y. (2016). Fluorescent nanoprobes for sensing and imaging of metal ions: Recent advances and future perspectives. *Nano today*, 11(3):309–329.

Zulehner, W. (2000). Historical overview of silicon crystal pulling development. *Materials Science and Engineering: B*, 73(1-3):7–15.

Zuo, J. M. and Spence, J. C. (2017). *Advanced transmission electron microscopy*. Springer.